Low-temperature heat capacity of antiferromagnetic ternary rare-earth iron silicides $M_2Fe_3Si_5$

C. B. Vining and R. N. Shelton
Ames Laboratory and Department of Physics, Iowa State University, Ames, Iowa 50011
(Received 7 February 1983)

The low-temperature heat capacity of antiferromagnetic ternary iron silicides $M_2Fe_3Si_5$ (M=Sm, Gd–Yb) has been measured from 0.5 to 30 K. Antiferromagnetic ordering temperatures range from 1.06 to 10 K for these materials including multiple magnetic transitions in $Sm_2Fe_3Si_5$, $Tb_2Fe_3Si_5$, and $Er_2Fe_3Si_5$. Magnetic ordering via the Ruderman-Kittel-Kasuya-Yosida interaction is indicated, even in the presence of large crystalline electric field effects. Entropy considerations indicate the magnetic ground state is a doublet in all of these materials except $Gd_2Fe_3Si_5$. Anomalous behavior is observed with respect to spin-wave and nuclear contributions to the total heat capacity, crystalline electric field effects, and critical behavior.

I. INTRODUCTION

Much attention has been focused on the competition between superconductivity and magnetism observed in several ternary rare-earth compounds.[1] Even in the absence of superconductivity, however, a complete understanding of the nature of the magnetic order in many of these compounds is still lacking. Particular attention has been given to the anomalous magnetic ordering temperatures in the MRh_4B_4 compounds[2] and the striking mean-field-like ferromagnetic transition observed in $HoRh_4B_4$.[3] The recent discovery of superconductivity and magnetism in the $M_2Fe_3Si_5$ compounds[4] presents another ternary system in which the superconducting and magnetic properties depend strongly on the choice of the rare earth M.

Mössbauer studies on $M_2Fe_3Si_5$ compounds utilizing the ^{57}Fe resonance[5–7] indicate the iron atoms carry no magnetic moment in either of the two crystallographically distinct Fe sites. Mössbauer measurements using the ^{161}Dy resonance in $Dy_2Fe_3Si_5$ indicate[6] a magnetic moment at the Dy site ($7.0\mu_b$) which is significantly reduced from the free-ion value ($10.6\mu_b$). Antiferromagnetic order, as determined by susceptibility measurements, has been observed for $M_2Fe_3Si_5$ compounds with M=Gd–Tm.[7] Observation of a commensurate-incommensurate antiferromagnetic transition by neutron diffraction in $Tb_2Fe_3Si_5$ (Ref. 8) and the possibility of reentrant superconductivity in $Tm_2Fe_3Si_5$ (Ref. 9) provided motivation for our present study of the low-temperature heat capacity of the $M_2Fe_3Si_5$ (M=Sc, Y, Sm, Gd–Lu) compounds as a means of better understanding the nature of the superconductivity and magnetic order in these materials. The low-temperature heat-capacity data of the magnetically ordered $M_2Fe_3Si_5$ compounds (M=Sm, Gd–Yb) are reported here as part of a systematic study of ternary rare-earth iron silicides. A parallel study of the low-temperature heat capacity of the superconducting compounds $Lu_2Fe_3Si_5$, $Sc_2Fe_3Si_5$, and $Y_2Fe_3Si_5$ has been reported previously.[10]

II. EXPERIMENTAL DETAILS

Samples of $M_2Fe_3Si_5$ (M=Sm, Gd–Tm) were prepared by arc melting stoichiometric mixtures of the elements in a Zr-gettered high-purity argon atmosphere followed by successive heat treatments at 1200 °C, 1000 °C, and 800 °C for two days each in quartz ampoules filled with an argon partial pressure of 150 Torr. Following this treatment, the sample of $Sm_2Fe_3Si_5$ showed physical deformation and assumed the shape of the quartz ampoule. This observation indicates the melting point of $Sm_2Fe_3Si_5$ is at or below 1200 °C. No indication of melting was observed in any of the other samples following this heat treatment. The sample of $Yb_2Fe_3Si_5$ was prepared in a somewhat different manner due to the relatively low boiling point and high vapor pressure of Yb. A nearly single-phase sample of $Yb_2Fe_3Si_5$ was produced by arc melting a eutectic composition of iron and silicon (20.5 at. % Si) with an excess of Yb over that required for a stoichiometric sample. This procedure was followed by melting in an additional amount of Si to achieve the stoichiometric composition. A sample in this "as-cast" form was chosen for use in the heat-capacity measurements since the annealing process resulted in a significant loss of Yb.

Powder x-ray diffraction patterns indicate all samples are single phase with lattice parameters in good agreement with previous results.[4] Low-frequency ac inductance measurements indicate antiferromagnetic ordering temperatures also in good agreement with previous results.[7] Details of the low-temperature heat-capacity measurement technique may be found in Ref. 10.

III. RESULTS

We first discuss our results for the low-temperature heat capacity of each of the eight compounds $M_2Fe_3Si_5$ (M=sm, Gd–Yb) on an individual basis and then point out trends observed throughout the series. In each case the total heat capacity, after correcting for the addenda in the usual way,[10] is expressed as

$$C = C_n + C_m + C_e + C_l \,, \tag{1}$$

where C_n is the nuclear contribution arising from the interaction of the nucleus with the effective magnetic field at the nucleus, C_m is the magnetic contribution arising from the electrons in the unfilled $4f$ shell of the rare-earth ions (assuming no direct contribution from the iron ions), C_e is the usual electronic contribution, and C_l is the lattice contribution.

For each sample in this study, the electronic and lattice contributions to the heat capacity are assumed to be identical to that found in $Lu_2Fe_3Si_5$.[10] A parametrization of the normal state heat capacity of $Lu_2Fe_3Si_5$ has therefore been subtracted from the heat capacity of each sample reported here. Thus in the following discussion, unless otherwise specified, the heat capacity referred to is given by

$$\Delta C = C - C_e(\mathrm{Lu}) - C_l(\mathrm{Lu}) = C_n + C_m \,, \tag{2}$$

where (Lu) refers to the appropriate values for $Lu_2Fe_3Si_5$. This assumption appears reasonable for all eight samples considered.

Several of these materials exhibit a relatively large nuclear Schottky anomaly. The contribution to the heat capacity from a nuclear Schottky anomaly at temperatures well above the maximum in the anomaly is expected to behave like

$$C_n/R = C_2/T^2 \,, \tag{3}$$

where C_2 is related to the effective magnetic field at the nucleus, H_{eff}, by

$$C_2 = \tfrac{1}{3}(\mu H_{\mathrm{eff}}/kI)^2 I(I+1) \,, \tag{4}$$

where μ is the effective magnetic moment of the nucleus, k is Boltzmann's constant, and I is the nuclear spin.[11]

The magnetic contribution to the heat capacity near the critical temperature is expected to behave as

$$C_m = A\,|\,1 - T/T_M\,|^{-\alpha} \,, \tag{5}$$

where α is a small positive number. In the limiting case of $\alpha \to 0$ the alternate form

$$C_m = A \ln|\,1 - T/T_M\,| \tag{6}$$

may be more applicable.[12] Well below the magnetic ordering temperature, the magnetic heat capacity can often be characterized by simple power laws or exponentials. An isotropic three-dimensional antiferromagnet, for example, is expected to have a spin-wave contribution to the heat capacity proportional to T^3.[11] The applicability of these various forms to our experimental results will be discussed in Sec. IV F.

Each of the Figs. 1–8 presents the low-temperature heat capacity of one of the eight samples discussed above. In each case, the heat capacity obtained in the manner discussed above is plotted in units of R (8.314 J), the molar gas constant, per mole of rare-earth (RE) atoms. Thus one mole of $Sm_2Fe_3Si_5$ contains two moles of the rare earth, Sm in this case. In each case, the entropy obtained by numerically integrating the heat capacity

$$S = \int (C/T)\,dT \tag{7}$$

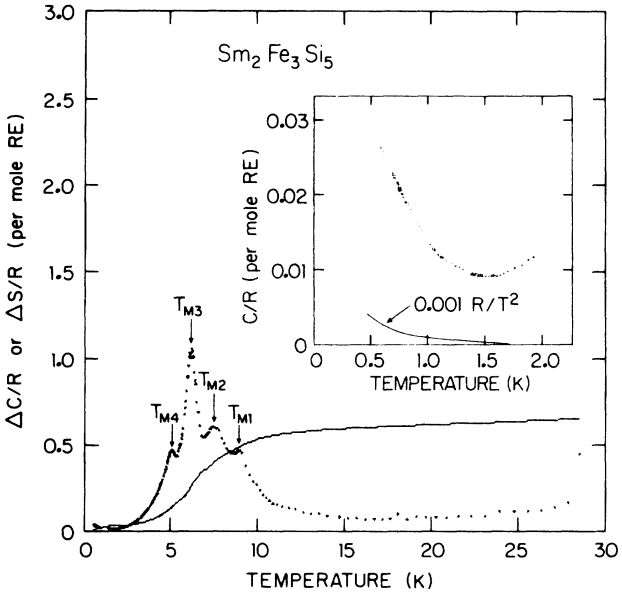

FIG. 1. Magnetic contribution to the heat capacity and entropy for $Sm_2Fe_3Si_5$. The inset indicates the nuclear Schottky anomaly expected for Sm metal (solid line) and the observed heat capacity of $Sm_2Fe_3Si_5$ below 2 K.

is also plotted in the same units. The lower limit of the integration is taken as the lowest temperature obtained rather than zero kelvin, but in most cases the error introduced by this procedure is less than one percent.

The low-temperature heat capacity and entropy of $Sm_2Fe_3Si_5$ from 0.5 to 30 K are presented in Fig. 1. The four distinct maxima at 5.05, 6.19, 7.35, and 8.96 K indicate four magnetic phase transitions. This is in contrast

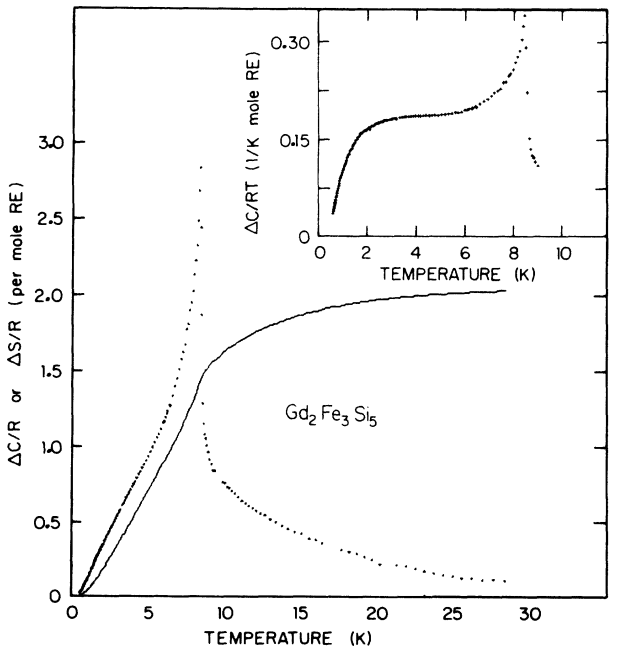

FIG. 2. Magnetic contribution to the heat capacity and entropy for $Gd_2Fe_3Si_5$. The inset indicates a large linear contribution to the heat capacity of $Gd_2Fe_3Si_5$ between 2 and 6 K.

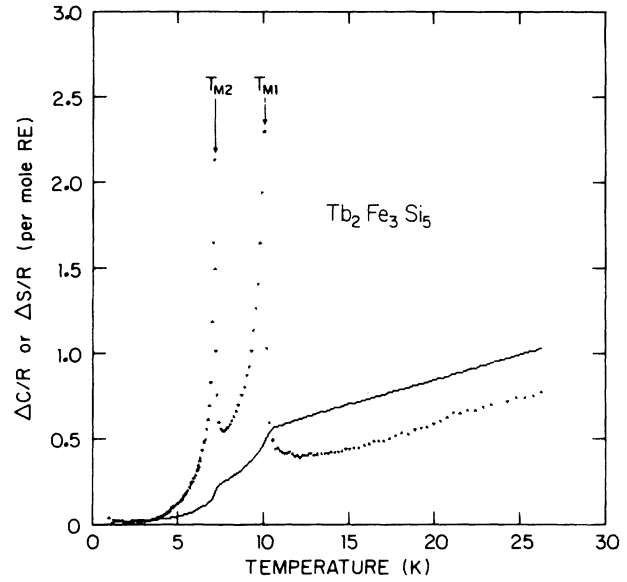

FIG. 3. Magnetic contribution to the heat capacity and entropy for $Tb_2Fe_3Si_5$.

to the complete absence of features in the susceptibility as determined by low-frequency ac inductance techniques both on this sample and on a sample studied previously.[13] The absence of any large change in susceptibility, together with the features evident in the heat capacity indicate the ordering at each of the peaks in the heat capacity is antiferromagnetic as reported previously for most of the other $M_2Fe_3Si_5$ compounds.[7] The entropy shows a distinct plateau well above all the transitions at $\Delta S=0.62R\approx R\ln 2$.

The inset of Fig. 1 indicates an increase in the heat capacity below 1 K, apparently due to the high-temperature side of a nuclear Schottky anomaly which should behave like Eq. (3) well above the maximum in the Schottky anomaly. From a graph of ΔC vs $1/T^2$, C_2 is estimated to be $0.014R\ \mathrm{K}^2$. Using the above value of C_2, $I=\frac{7}{2}$, $\mu=0.4\mu_N$, and Eq. (4), an effective field of 12 MG at the Sm nucleus, is calculated. An effective field typical of Sm metal derived in a similar manner is 3.3 MG,[11] much lower than the value for this ternary silicide. Indeed, a nuclear anomaly typical of Sm metal, indicated by the solid line in the inset to Fig. 1, should be quite small and nearly unobservable at the lowest temperatures reached in this experiment. The possible origin of such a large effective field is considered in Sec. IV E.

The low-temperature heat capacity and entropy of $Gd_2Fe_3Si_5$ are presented in Fig. 2. A single prominent peak is evident in the heat capacity at 8.40 K. As expected, there is no indication of a nuclear anomaly for Gd. There is, however, an inflection in the heat capacity below the antiferromagnetic ordering temperature. A plateau from about 2.5 to 6.5 K in a plot of $\Delta C/RT$ against temperature shown in the inset in Fig. 2 indicates the heat capacity has a large linear term in this temperature range. The possible origin of such a large linear term and its relation to spin waves will be discussed in Sec. IV F. The entropy at 28 K is $\Delta S=2.02R$, in excellent agreement with the total entropy expected, i.e., $R\ln(2J+1)=R\ln 8=2.08R$.

The low-temperature heat capacity and entropy of $Tb_2Fe_3Si_5$ are presented in Fig. 3. Two large peaks are observed in the heat capacity at 10.02 and 7.06 K, in excellent agreement with previous susceptibility and neutron-diffraction results.[7,8] Neutron-diffraction results indicate a transition at 10 K to an antiferromagnetically ordered state in which the magnetic structure is incommensurate with the lattice. This state is followed by a second transition at 7 K to a different antiferromagnetically ordered

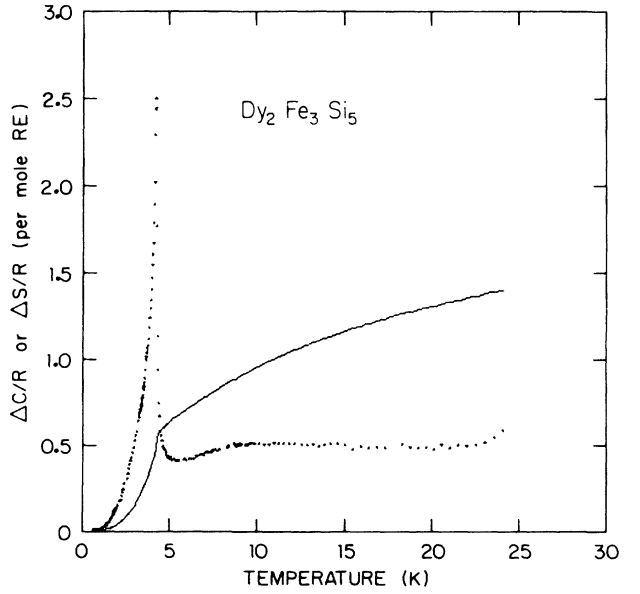

FIG. 4. Magnetic contribution to the heat capacity and entropy for $Dy_2Fe_3Si_5$.

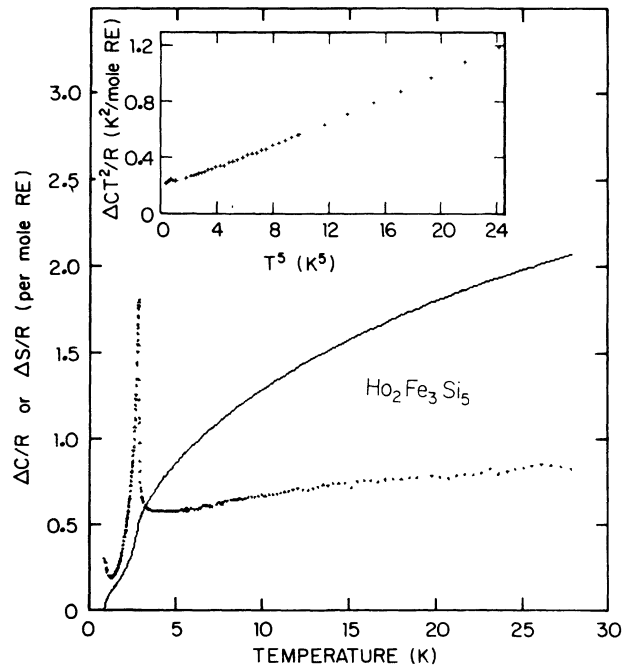

FIG. 5. Magnetic contribution to the heat capacity and entropy for $Ho_2Fe_3Si_5$. The inset indicates the nuclear Schottky anomaly below 1.8 K (see Secs. III E and IV E for details).

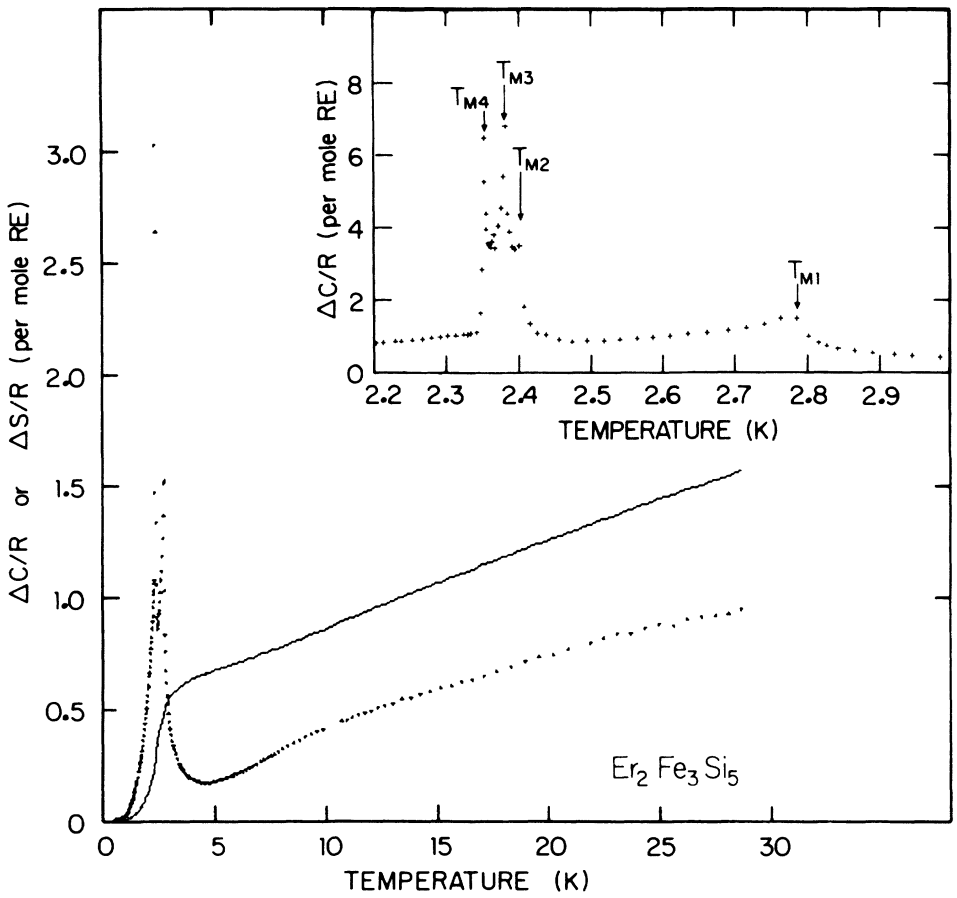

FIG. 6. Magnetic contribution to the heat capacity and entropy for $Er_2Fe_3Si_5$. The inset indicates the magnetic contribution to the heat capacity for $Er_2Fe_3Si_5$ between 2.2 and 3.0 K. Note the change of scale.

state which is commensurate with the lattice.[8] At the lowest temperatures attained, a slight upturn in the heat capacity with decreasing temperature reveals the presence of a nuclear Schottky anomaly expected for Tb. While lower temperatures would be needed for a quantitative comparison, the magnitude of this anomaly is in qualitative agreement with that expected for Tb metal.

The low-temperature heat capacity and entropy of $Dy_2Fe_3Si_5$ are presented in Fig. 4. One large peak is evident at 4.20 K indicating the onset of antiferromagnetic order consistent with previous susceptibility results. This peak is much steeper on the high-temperature side than on the low-temperature side of the maximum. This asymmetry will be discussed in detail in Sec. IV D. Above the ordering temperature, the heat capacity remains near $0.4R$ per mole of RE atoms, exhibiting a broad maximum near 9 K.

The low-temperature heat capacity and entropy of $Ho_2Fe_3Si_5$ are presented in Fig. 5. The heat capacity of this sample is remarkably similar in many respects to the heat capacity of $Dy_2Fe_3Si_5$. One large peak is evident in the heat capacity at 2.82 K, indicating the onset of antiferromagnetic order consistent with previous susceptibility results. The peak at 2.82 K is quite asymmetric and, as for $Dy_2Fe_3Si_5$, much steeper on the high-temperature side than on the low-temperature side. Above the ordering temperature, the heat capacity remains large ($\sim 0.6R$) and increases slowly with temperature to 28 K. Below 2 K the heat capacity increases with decreasing temperature as expected qualitatively for the nuclear Schottky anomaly associated with the Ho nucleus. The inset to Fig. 5 shows the data at temperatures below the minimum in the heat capacity ($T < 1.9$ K). From this plot, an estimate of the coefficient C_2 in Eq. (3) may be made for the nuclear Schottky contribution. Specifically, if the magnetic contribution goes like T^3 as expected for an isotropic three-dimensional antiferromagnetic spin wave, then the intercept in the inset of Fig. 5 will represent the coefficient C_2 in the nuclear contribution to the heat capacity. The value for C_2 resulting from this is $C_2 = 0.18R$. Using $I = \frac{7}{2}$, $\mu = 4.08\mu_N$, and Eq. (4) the effective field at the Ho nucleus is estimated to be 4.3 MG, compared to an effective field of 7.5 MG calculated in a similar manner for Ho metal.[11]

The low-temperature heat capacity and entropy of $Er_2Fe_3Si_5$ are presented in Fig. 6. Large peaks are evident in the heat capacity at 2.35 and 2.78 K in this figure. The data between 2.2 and 3.0 K are presented in the inset to Fig. 6 on an expanded temperature scale and a compressed heat-capacity scale as compared with Figs. 1–8. The feature marked T_{M1} in the inset at 2.78 K is the smaller of the two peaks evident in the main figure. The magnitude of the feature at 2.35 K is more than a factor of 2 larger than any of the other features observed in this system of

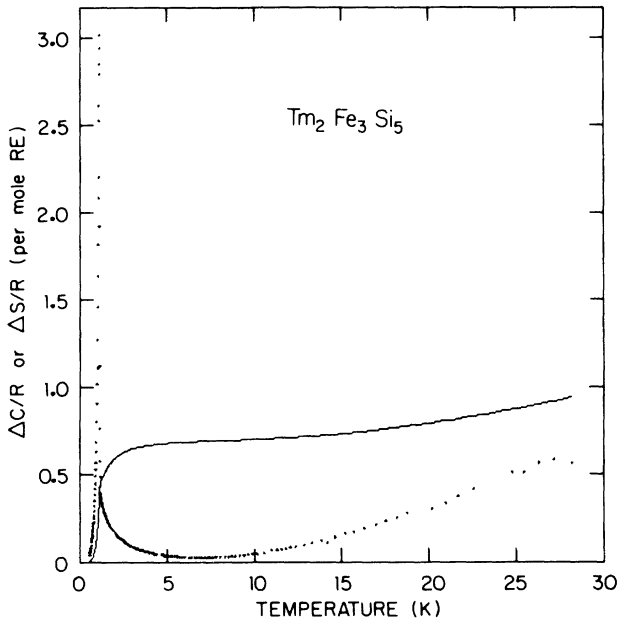

FIG. 7. Magnetic contribution to the heat capacity and entropy for $Tm_2Fe_3Si_5$.

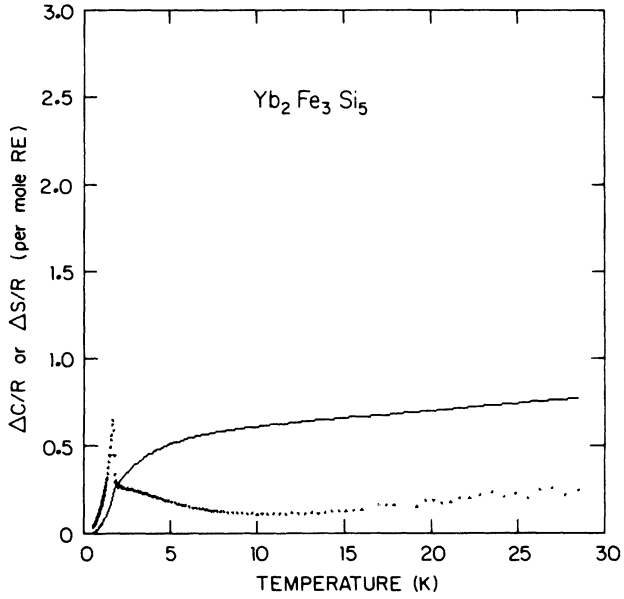

FIG. 8. Magnetic contribution to the heat capacity and entropy for $Yb_2Fe_3Si_5$.

compounds. This feature is extremely sharp in temperature with a total width of less than 75 mK. There are two clear peaks in this feature at 2.352 K (T_{M4}) and 2.381 K (T_{M3}). A shoulder at 2.401 K defined by only two points is also indicated by T_{M2} in the inset. These data were taken in four successive runs and in two different experiments, eight weeks apart. The excellent agreement attests to the reproducibility of these magnetic phenomena. The average interval between data points in the region of the features at 2.3–2.4 K is less than 3 mK. Finer resolution might resolve more clearly the peak at T_{M2}. Note that the heat capacity in the region from 2.2 to 2.35 K which appears essentially constant in the inset to Fig. 6 is in reality a rapidly increasing function of temperature as can be seen by comparison to the main figure. The sharp rise in the heat capacity on the low-temperature side of T_{M4} can be identified in the main figure by the sudden change in the density of data points near 2.3 K. The data rapidily rise from near $1.1R$ just below T_{M4} to well off the scale of the main figure.

The heat capacity above the ordering temperatures drops to $0.15R$ near 4.5 K and then rises for temperatures above this point. At the very lowest temperatures the heat capacity begins to rise with decreasing temperatures, indicating a nuclear Schottky anomaly. Lower temperatures would be required for a quantitative estimate of the temperature dependence of this anomaly; however, the size of the feature is in qualitative agreement with the anomaly observed in Er metal.

The low-temperature heat capacity and entropy for $Tm_2Fe_3Si_5$ are presented in Fig. 7. A large peak in the heat capacity is evident at 1.06 K indicating the onset of antiferromagnetic order. The heat capacity decreases above 1.06 K with increasing temperature until 7 K, after which it again increases. The entropy shows a plateau at about $0.69R \approx R \ln 2$ from 2 to 10 K reflecting the small heat capacity in this region. Attempts to fit the low-temperature side of the peak in the heat capacity to a logarithmic divergence as given by Eq. (6) resulted in an unreasonably large value for T_M suggesting that the heat capacity may be finite at the antiferromagnetic ordering temperature. Possible reasons for this will be discussed in Sec. IV D.

The low-temperature heat capacity and entropy for $Yb_2Fe_3Si_5$ are presented in Fig. 8. A peak in the heat

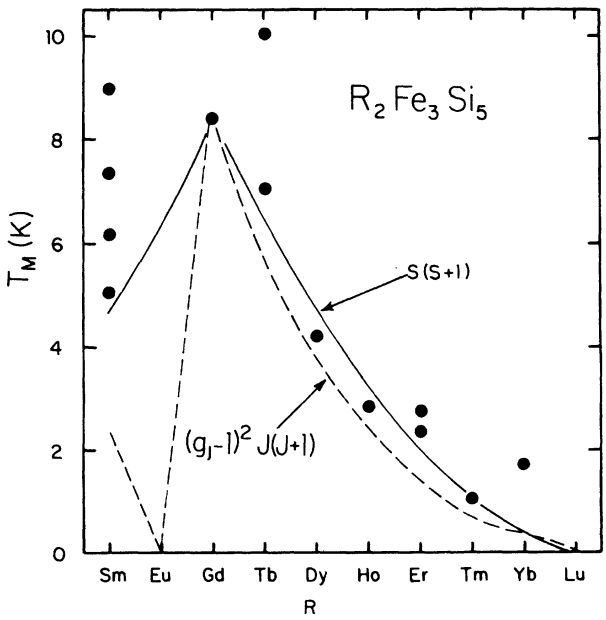

FIG. 9. Magnetic ordering temperatures for $M_2Fe_3Si_5$ compounds. The solid line indicates ordering temperatures expected if the effective moment on M varies as S and the dashed line indicates the ordering temperatures expected if the effective moment varies as J.

TABLE I. Magnetic properties of rare-earth ternary iron silicides. Entropy is in units of R per mole of rare earth.

Compound	T_M (K)[a]	T_M (K)[b]	$S(T_M)/R$	J	$\ln(2J+1)$	$S(28\ \text{K})/R$
$Yb_2Fe_3Si_5$	1.70		0.20[c]	$\frac{7}{2}$	2.08	0.77[c]
$Tm_2Fe_3Si_5$	1.06	1.13[d]	0.35	6	2.56	0.938
$Er_2Fe_3Si_5$	2.79	2.85[e]	0.50	$\frac{15}{2}$	2.77	1.55
	2.401	2.55[e]	0.325			
	2.381		0.286			
	2.352		0.237			
$Ho_2Fe_3Si_5$	2.82	2.9[f]	0.44[g]	8	2.83	2.03
$Dy_2Fe_3Si_5$	4.20	4.4[f]	0.50	$\frac{15}{2}$	2.77	1.40
$Tb_2Fe_3Si_5$	10.02	10.3[h]	0.51	6	2.56	1.03
	7.06	7[h]	0.15			
$Gd_2Fe_3Si_5$	8.40	8.6[f]	1.42	$\frac{7}{2}$	2.08	2.02
$Sm_2Fe_3Si_5$	8.96		0.49	$\frac{5}{2}$	1.79	1.29
	7.35		0.38			
	6.19		0.26			
	5.05		0.14			

[a]This work.
[b]Previously reported.
[c]After correcting for Yb weight loss (see Sec. II).
[d]Reference 9.
[e]Reference 14.
[f]Reference 7.
[g]After correcting for the nuclear contribution (see Sec. IV).
[h]Reference 8.

capacity at 1.70 K indicates the onset of antiferromagnetic order. The heat capacity decreases with increasing temperature above the ordering temperature of 1.70 K until 10 K where the heat capacity begins to increase with increasing temperature. The increase at higher temperatures is attributed to an electronic Schottky anomaly due to the crystalline electric field (CEF) splitting of the $4f$ shell of Yb. The appearance of magnetic order indicates that Yb is in a trivalent state in this compound rather than the more common, nonmagnetic divalent state. The trivalent state for Yb is also indicated by the lattice parameters for $Yb_2Fe_3Si_5$ when compared to other members of the $M_2Fe_3Si_5$ series.[4]

A relatively flat region in the entropy from 8 to 15 K near the value $0.68R \approx R \ln 2$ indicates the magnetic ground state in $Yb_2Fe_3Si_5$ is a doublet. The heat capacity above the magnetic ordering temperature exhibits negative curvature from 1.7 to about 3 K and the general shape is suggestive of a Schottky anomaly. Indeed the entropy at the transition is only $0.2R$, much lower than that expected for a doublet, the simplest degenerate ground state. This suggests that the magnetic ground state consists of two closely spaced singlets, with the next excited state at a considerably higher temperature.

IV. DISCUSSION

A. Ordering temperatures

Having briefly discussed the low-temperature heat capacity of each of the members of the series $M_2Fe_3Si_5$ we now turn our attention to some of the systematic trends observed in these data. Figure 9 and Table I present the ordering temperatures for each of the $M_2Fe_3Si_5$ compounds (M=Sm–Yb, except Eu which does not form a ternary compound in this structure). More than one transition temperature is indicated for $Sm_2Fe_3Si_5$, $Tb_2Fe_3Si_5$, and $Er_2Fe_3Si_5$ as discussed in Sec. III. The lower transition for $Er_2Fe_3Si_5$ indicated in Fig. 9 actually represents the closely spaced group T_{M2}, T_{M3}, and T_{M4} as designated in Fig. 6. The magnetic ordering temperatures for a series of isostructural and isoelectronic metals where the indirect Ruderman-Kittel-Kasuya-Yosida (RKKY) exchange interaction is the main interaction between the magnetic moments are expected to scale as $S(S+1)$ where S is the spin of the local moment or in the case where L, the orbital angular momentum, is not quenched as $(g_J-1)^2J(J+1)$ where g_J is the Landé g factor and J is the total angular momentum of the local moment. The latter case is more usual for the rare-earth elements.

The solid line in Fig. 9 represents the ordering temperatures expected for the series $M_2Fe_3Si_5$ normalized to the observed ordering temperature in $Gd_2Fe_3Si_5$ for the case where S is a good quantum number. The dashed line is similarly normalized to the observed ordering temperature of $Gd_2Fe_3Si_5$ and gives the expected ordering temperatures for the case where J is a good quantum number. Considering only those compounds for which one ordering temperature is observed, $Gd_2Fe_3Si_5$, $Dy_2Fe_3Si_5$, $Ho_2Fe_3Si_5$, $Tm_2Fe_3Si_5$, and $Yb_2Fe_3Si_5$, either of the two curves gives reasonable agreement between the expected and observed magnetic ordering temperatures. Of this group only $Yb_2Fe_3Si_5$ lies far from the theoretical curves. This may be related either to the significant splitting of the ground-

state doublet in this compound or to mixed-valence effects, often observed in Yb compounds.

Those compounds exhibiting multiple transitions, $Sm_2Fe_3Si_5$, $Tb_2Fe_3Si_5$, and $Er_2Fe_3Si_5$, have transition temperatures falling considerably above either of these curves. In each case, however, the lowest transition is reasonably close to the $S(S+1)$ curve. The rough agreement between the ordering temperatures and the trend predicted by the $S(S+1)$ curve or the $(g_J-1)^2J(J+1)$ (the de Gennes factor) curve, particularly for the heavy rare-earth compounds M=Gd—Tm, indicates the major mechanism responsible for the magnetic ordering in these compounds is the usual RKKY indirect exchange interaction. In particular, there is no evidence in our data to indicate dipole-dipole interactions are important, as has been suggested for these compounds.[7] Furthermore, the full moment or some effective moment which varies nearly as J (or perhaps S) determines the ordering temperatures in these compounds.

B. Coupling constants

In mean-field theory the inter-rare-earth coupling constant J' is related to the magnetic ordering temperature by

$$T_M = 2\mathcal{J}'S(S+1)z/3k \tag{8}$$

when S is a good quantum number and by

$$T_M = 2\mathcal{J}'(g_J-1)^2J(J+1)z/3k \tag{9}$$

when J is a good quantum number where z is the number of nearest-neighbor M atoms.[2] Strictly speaking there are only two nearest-neighbor M atoms in this structure due to the low symmetry of the M site; however, two additional M atoms are positioned at M-M distances only about 1% greater than for the two nearest neighbors. Therefore, using $z=4$ to account for these four "nearest-neighbor" M atoms, the ordering temperature of $Gd_2Fe_3Si_5$ ($T_M=8.40$ K), $J=\frac{7}{2}$, and $g_J=2$ yields $\mathcal{J}'=1.7\times10^{-5}$ eV.

The depression of the supcerconducting transition temperature of $Lu_2Fe_3Si_5$ by Gd impurities in $(Lu_{1-x}Gd_x)_2Fe_3Si_5$ can be used to estimate $\mathcal{J}$, the conduction-electron—M exchange coupling constant. In the theory of Abrikosov and Gorkov, the depression of the superconducting transition temperaure is related to the concentration of magnetic impurities in the limit of low impurity concentration, by

$$\frac{dT_c}{dn} = \frac{5dT_c}{dx} = -\frac{\pi^2N(0)}{2k}\mathcal{J}^2(g_J-1)^2J(J+1)\,, \tag{10}$$

where dT_c/dn is the rate of depression of T_c per atomic percent impurity, dT_c/dx is the rate of depression of T_c per atomic fraction of Gd in Lu and $N(0)$ is the density of states at the Fermi level.[2] Using $(dT_c/dx)/[(g_J-1)^2J(J+1)]=4.9$ K per atom fraction Gd from Ref. 13 and $N(0)=0.59$ states/eV atom spin from Ref. 10, $\mathcal{J}$ is estimated to be 2.7×10^{-2} eV. To order of magnitude $\mathcal{J}$ and $\mathcal{J}'$ are related by[2]

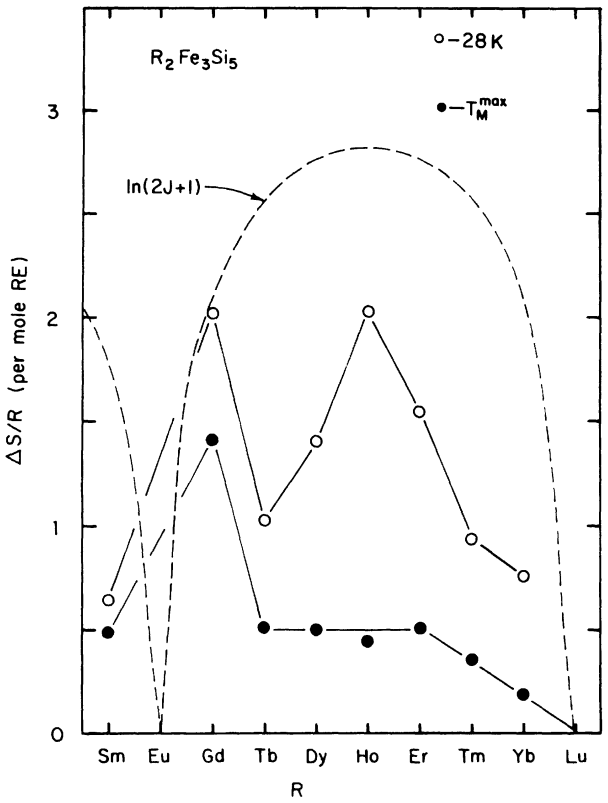

FIG. 10. Magnetic contribution to the entropy for $M_2Fe_3Si_5$ compounds. The open circles indicate the entropy observed at 28 K and the solid circles indicate the entropy observed at the highest magnetic ordering temperature for each compound.

$$\mathcal{J} \approx [\mathcal{J}'N(0)]^{1/2}\,. \tag{11}$$

Using $\mathcal{J}'$ derived above from the ordering temperature of $Gd_2Fe_3Si_5$ yields $\mathcal{J}=5.4\times10^{-3}$ eV. This is in reasonable agreement with the estimate from the superconducting data, especially considering the crude nature of these estimates. Both estimates suggest the conduction-electron—M coupling is strong enough to mediate the indirect exchange interaction as has been previously reported for the MRh_4B_4 compounds.[2]

C. CEF effects

Figure 10 and Table I present the entropy observed at the highest magnetic transition (when there is more than one transition temperature) for each of the eight compounds discussed in Sec. III as well as the entropy at 28 K for each compound. The dashed line represents the entropy for each compound assuming a total angular momentum J given by Hund's rules. The entropy associated with the nuclear Schottky anomaly in $Ho_2Fe_3Si_5$ has been neglected for the purposes of this figure. Only $Gd_2Fe_3Si_5$ exhibits nearly the full entropy at 28 K available from the total quantum number $J=\frac{7}{2}$. This is expected for Gd compounds, since $L=0$ in this case and CEF effects are therefore absent to first order. Considerably higher temperatures than attained in these experiments would be needed to observe all the entropy available from the full Hund's-rules value of J in each of the other compounds.

This indicates that CEF effects are indeed quite important in these compounds, in agreement with previous susceptibility and Mössabuer results.[6,7] For the compounds with non-S state rare-earth elements (i.e., excluding $Gd_2Fe_3Si_5$) the entropy at 28 K peaks at $Ho_2Fe_3Si_5$ with $J=8$, the largest value of the total angular momentum.

In five of these compounds $Sm_2Fe_3Si_5$, $Tb_2Fe_3Si_5$, $Dy_2Fe_3Si_5$, $Ho_2Fe_3Si_5$, and $Er_2Fe_3Si_5$ the entropy at the transition is very nearly $0.5R$ (see Fig. 10). This is especially surprising since the number of transitions observed varies from one transition ($Dy_2Fe_3Si_5$) to four transitions ($Sm_2Fe_3Si_5$). The amount of entropy below the transition is very nearly the value predicted by a three-dimensional Ising model ($0.511R$) for spin-$\frac{1}{2}$ systems on a diamond lattice ($z=4$).[12] This indicates that in each of these five compounds, the magnetic ground state is a doublet as compared to the considerably higher degeneracy expected from Hund's rules. The doublet ground state is directly observed in $Sm_2Fe_3Si_5$ where the entropy indicates (Fig. 1) that the next excited state is considerably higher than the ordering temperature.

In $Tm_2Fe_3Si_5$ (Fig. 7) and $Yb_2Fe_3Si_5$ (Fig. 8), the entropy also suggests the ground state is a doublet. In both cases, the entropy below the ordering temperature is well below $0.5R$ indicating a large fraction of the R ln(2) of entropy is contained in the high-temperature tail occurring above the ordering temperature. This suggests that the doublet is not entirely degenerate. Indeed the heat capacity above the ordering temperature in $Yb_2Fe_3Si_5$ appears similar to that expected from a two-level Schottky anomaly. This implies the CEF effects are sufficiently large to split the doublets, presumably via the spin-orbit coupling.

D. Critical behavior

As discussed in Sec. III, the peak in the heat capacity of several of these compounds is very asymmetric, appearing steeper on the high-temperature side than on the low-temperature side. Figure 11 presents the heat capacity near the magnetic ordering temperatures for three of these samples, $Dy_2Fe_3Si_5$, $Ho_2Fe_3Si_5$, and $Er_2Fe_3Si_5$, both above and below the ordering temperatures. In the case of $Er_2Fe_3Si_5$, only the highest ordering temperature (T_{M1}) is considered. A logarithmic divergence such as described by Eq. (6) will appear as a straight line on such a plot and of the six lines in this figure only four are straight. Below the critical temperature, the data for $Dy_2Fe_3Si_5$ and $Ho_2Fe_3Si_5$ (solid circle and solid triangle, respectively, in Fig. 11) appear as straight lines and are nearly parallel to each other. The data for $Er_2Fe_3Si_5$ also appear to diverge logarithmically below T_{M1} as evidenced by the solid squares in Fig. 11.

Above the critical temperatures the situation is very different. The data for $Er_2Fe_3Si_5$ appear logarithmic as evidenced by the open squares in Fig. 11; however, there is pronounced curvature in the data above the critical temperatures for both $Dy_2Fe_3Si_5$ and $Ho_2Fe_3Si_5$. Above the critical temperatures, the data for $Dy_2Fe_3Si_5$ and $Ho_2Fe_3Si_5$ appear to diverge with a critical exponent of 1, that is

$$C=A(T/T_M-1)^{-1}+B=AT_M/(T-T_M)+B \quad (12)$$

as indicated in Fig. 12 where we plot heat capacity versus $T_M/(T-T_M)$. The same critical temperatures are used in this figure as are used in Fig. 11. Again the curves for $Dy_2Fe_3Si_5$ and $Ho_2Fe_3Si_5$ appear very similar to each other and qualitatively different from the curve for $Er_2Fe_3Si_5$. These two plots clearly indicate that the highest transition in $Er_2Fe_3Si_5$ is typical of second-order phase transitions, showing a nearly logarithmic divergence both above and below T_{M1}, while $Dy_2Fe_3Si_5$ and $Ho_2Fe_3Si_5$ show qualitatively different critical behavior and perhaps exhibit dif-

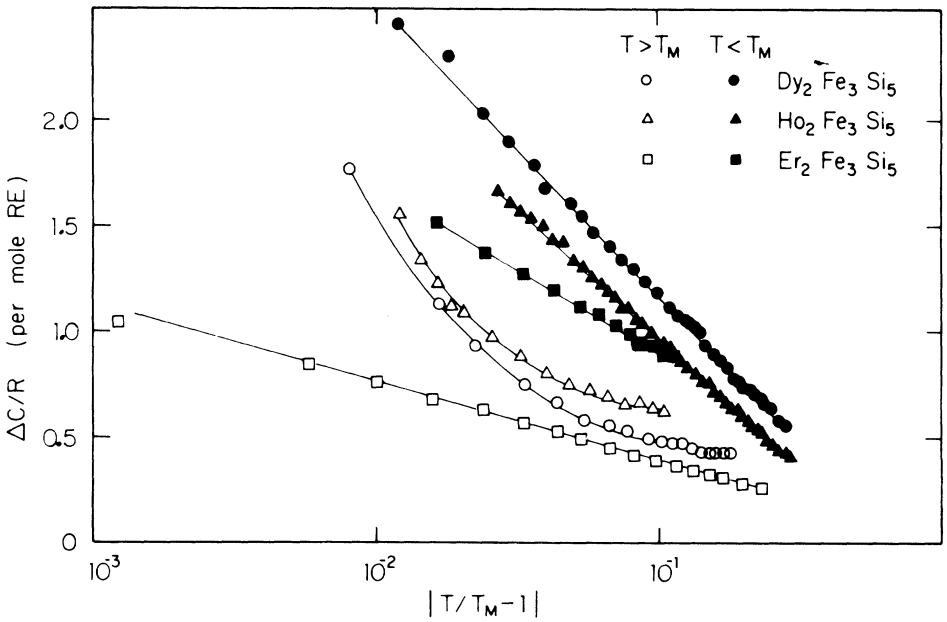

FIG. 11. Magnetic contribution to the heat capacity vs $|T/T_M-1|$ above (open symbols) and below (closed symbols) the magnetic ordering temperature for $Dy_2Fe_3Si_5$, $Ho_2Fe_3Si_5$, and $Er_2Fe_3Si_5$. For $Er_2Fe_3Si_5$, T_M refers to T_{M1} from Fig. 6. Note the logarithmic temperature scale.

ferent critical exponents above and below their critical temperatures.

As discussed in Sec. III, neither $Tm_2Fe_3Si_5$ nor $Yb_2Fe_3Si_5$ exhibits a clear logarithmic or even nearly logarithmic divergence either above or below its critical temperature, but rather suggests a finite maximum in the specific heat instead of a divergence. In the case of $Gd_2Fe_3Si_5$ and $Tb_2Fe_3Si_5$, the critical behavior is less clear due to a lower density of data points in this temperature range. $Sm_2Fe_3Si_5$ exhibits no sharp peaks in the heat capacity, but only more broadened maxima, especially when compared to the other seven compounds considered in this study. This may indicate sample inhomogeneities related to the lower melting point of this compound and the heat treatment of this sample. Inhomogeneities may also play a role in the critical behavior of $Yb_2Fe_3Si_5$ which was not annealed due to the low melting point of Yb.

The lower transitions in $Er_2Fe_3Si_5$, T_{M2}, T_{M3}, and T_{M4}, would appear to be of the first order as indicated both by the huge magnitude of these heat-capacity spikes and the sharp onset and completion of the transitions. Very sharp features are also observed near 2.35 K in low-frequency inductance and resistivity measurements performed on this compound. Similarly, the lower transition in $Tb_2Fe_3Si_5$ is quite sharp and although the resolution of the heat-capacity data is not as good for this compound, this may also be a first-order transition.

E. Nuclear Schottky anomalies

Several of these compounds exhibit a detectable nuclear Schottky anomaly at the lowest temperatures reached. In two cases, the anomaly is of sufficient magnitude to permit a quantitative estimate of the coefficient of the $1/T^2$ term. As discussed in Sec. III, the nuclear Schottky anomaly in $Ho_2Fe_3Si_5$ appears to be only half as large as expected, whereas the anomaly in $Sm_2Fe_3Si_5$ appears to be an order of magnitude larger than expected from the respective rare-earth metals. This may be related to the CEF effects which can alter the effective moment of the rare earth and therefore the effective magnetic field experienced by the nucleus. The large nuclear anomaly observed in $Sm_2Fe_3Si_5$, however, is especially difficult to understand. In the rare-earth metals, the principal source of the effective field experienced by the nucleus is the orbital angular momentum L.[11] CEF effects are expected to have their principal effect on L, thus reducing the field experienced by the nucleus and thereby reducing the observed Schottky anomaly. The dramatic increase in the nuclear anomaly in $Sm_2Fe_3Si_5$ is therefore difficult to understand since CEF effects can be expected only to reduce the effective field at the nucleus.

F. Spin waves

The heat capacities of all eight compounds were examined graphically and numerically for indications of simple temperature dependences below the ordering temperatures. Functional forms such as simple power laws, exponential, logarithmic, and simple combinations of some of these forms were investigated with respect to the data below the respective transition temperatures. Various functional forms for the heat capacity seem more or less successful over limited temperature ranges; however, no consistent patterns or trends emerged from these efforts. In the case of $Gd_2Fe_3Si_5$ described in Sec. III, there is a significant linear term in the heat capacity below the magnetic ordering temperature. This large linear contribution is evident over an extended temperature range (see Fig. 2). A linear term in the heat capacity could be expected from two-dimensional ferromagnetic spin waves (where the magnon dispersion relation is proportional to q^2) or from one-dimensional antiferromagnetic spin waves (where the magnon dispersion relation is proportional to q). Since the magnetic structure of this compound is not known, one can only hypothesize about the spin-wave contributions to the heat capacity of $Gd_2Fe_3Si_5$.

V. CONCLUSIONS

The dependence of the antiferromagnetic ordering temperature on rare earths as depicted in Fig. 9 agrees reasonably well with the ordering temperatures predicted by the de Gennes factor. This is especially true if only the lowest transition is considered for those materials in which more than one ordering temperature is observed. In $Tb_2Fe_3Si_5$ (Ref. 8) and more recently $Er_2Fe_3Si_5$,[14] neutron-diffraction experiments indicate the antiferromagnetic structure at the lowest temperatures is commensurate with the lattice while the magnetic structures at higher temperatures are incommensurate with the lattice. The critical behavior of the heat capacities of $Dy_2Fe_3Si_5$, $Ho_2Fe_3Si_5$, and $Er_2Fe_3Si_5$ as discussed in Sec. III and presented in Figs. 11 and 12 further indicates the upper transition in compounds with multiple transitions is qualitatively dif-

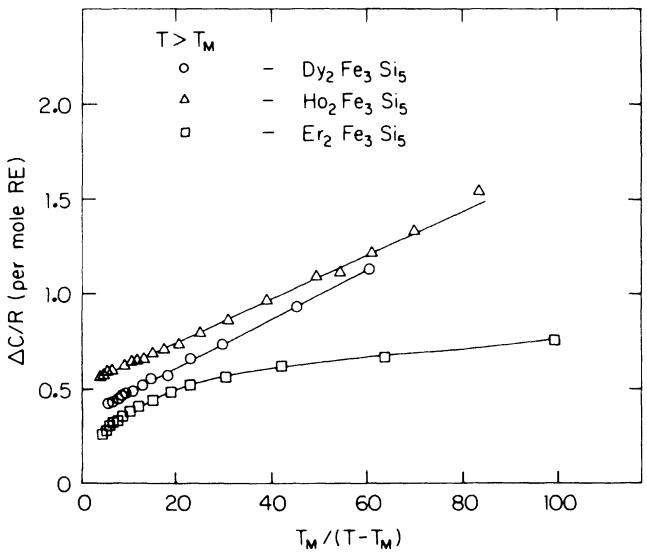

FIG. 12. Magnetic contribution to the heat capacity vs $T_M/(T-T_M)$ above the magnetic ordering temperature for $Dy_2Fe_3Si_5$, $Ho_2Fe_3Si_5$, and $Er_2Fe_3Si_5$.

ferent from the antiferromagnetic transition in those compounds with a single transition. Assuming the antiferromagnetic structure in each of the compounds with a single ordering temperature is also commensurate with the lattice, as seems likely, the ordering temperatures which should be compared to the de Gennes curve should be only the lowest ordering temperatures. In particular, there is no indication that dipole-dipole contributions play any significant role in determining the ordering temperatures as has been speculated.[7]

Figure 10 illustrates the large and systematic CEF effects in these compounds. In all cases except $Gd_2Fe_3Si_5$, a large fraction of the Hund's-rules entropy is not recovered by 28 K. For example, only 40% of the Hund's-rule entropy is recovered by 28 K in $Tb_2Fe_3Si_5$ and the fraction is even smaller in the case of $Yb_2Fe_3Si_5$. In five of these compounds, the entropy at the highest antiferromagnetic ordering temperature is very nearly $0.5R$. This indicates that the ground state in these cases is a doublet. Thus in each compound except $Gd_2Fe_3Si_5$, the ground state is split by the CEF to a doublet or in the case of $Tm_2Fe_3Si_5$ and $Yb_2Fe_3Si_5$ to two singlets within about 1 K. All other states lie at much higher temperatures. The doublet ground state occurs without regard to the number of electrons in the $4f$ shell, in particular without regard to whether the number of electrons is even or odd.

The low symmetry of the rare-earth site in this structure prohibits the development of a detailed energy-level scheme based on the data available; however, some conclusions can be drawn about the nature of the ground state. As discussed in Sec. III, the ground state in these compounds is a doublet. Mössbauer data on $Dy_2Fe_3Si_5$ indicate a moment on Dy in this compound of $7.0\mu_B$, reduced from the Hund's-rule value of $10.6\mu_B$. This indicates that the ground state is not made up of pure $|+\frac{15}{2}\rangle$ and $|-\frac{15}{2}\rangle$ states but includes some admixture of lower J_z states. This makes the nearly de Gennes–like behavior of the ordering temperatures all the more puzzling since the effective angular momentum of the ground-state doublet is expected to determine the ordering temperature and it is difficult to understand how, in general, any states other than the states of maximum J_z ($|\pm\frac{15}{2}\rangle$ in the case of $Dy_2Fe_3Si_5$) can produce an effective moment which varies in the same way as the Hund's-rule moment. Thus the de Gennes factor variation of the ordering temperatures is difficult to understand in view of the large CEF effects evident in these compounds.

Several distinctly different critical behaviors are observed in these compounds. Most striking is the set of transitions T_{M2}, T_{M3}, and T_{M4} in $Er_2Fe_3Si_5$ indicated in Fig. 6. The narrow width of these peaks and the sharpness of the high- and low-temperature sides of the feature as a whole indicate these are first-order phase transitions. Recent neutron-diffraction results indicate the feature at 2.34 K represents an incommensurate-commensurate magnetic transition.[14] The separate peaks in the heat capacity may represent ordering, as the temperature increases, to successively higher-order commensurate phases until finally the incommensurate phase dominates.

The heat capacities of $Dy_2Fe_3Si_5$ and $Ho_2Fe_3Si_5$ are quite similar, even on close inspection. The apparent difference in the critical exponents above and below the ordering temperature is clearly demonstrated in Figs. 11 and 12. Truly different critical exponents above and below the ordering temperature implies a discontinuity in the slope of the free energy and therefore a first-order phase transition. An alternative possibility is that the apparent critical exponent of $+1$ above the ordering temperature only results from the smearing, possibly due to sample inhomogeneities, of a discontinuity in the specific heat as expected in mean-field theories. In this case the apparent critical exponent of $+1$ above the ordering temperature must be viewed as coincidental and not of any intrinsic importance. Either of these possibilities is unusual.

$Sm_2Fe_3Si_5$, $Tm_2Fe_3Si_5$, and $Yb_2Fe_3Si_5$ exhibit what appear to be finite maxima in their heat capacities as compared to the singularities clearly observed in the heat capacities of $Dy_2Fe_3Si_5$, $Ho_2Fe_3Si_5$, and $Er_2Fe_3Si_5$ and probably the singularities observed in $Gd_2Fe_3Si_5$ and $Tb_2Fe_3Si_5$. The heat capacities of $Tm_2Fe_3Si_5$ and $Yb_2Fe_3Si_5$ do not appear to diverge logarithmically as discussed in Sec. III. $Sm_2Fe_3Si_5$ exhibits markedly rounded maxima in its heat capacity. Sample inhomogeneities may account for the finite maxima observed in the heat capacities of these compounds or the finite maxima may indicate mean-field-like behavior such as has been observed in $HoRh_4B_4$ and was suggested above for $Dy_2Fe_3Si_5$ and $Ho_2Fe_3Si_5$. $Yb_2Fe_3Si_5$ also exhibits anomalous curvature in its heat capacity above the magnetic ordering temperature. This may be attributed to an electronic Schottky-type anomaly arising from splitting of the ground-state doublet in this compound.

Nuclear Schottky anomalies are observed in $Sm_2Fe_3Si_5$ and $Ho_2Fe_3Si_5$ which are larger and smaller, respectively, than expected from the observed anomalies in the respective rare-earth metals.[11] In the case of $Sm_2Fe_3Si_5$ the discrepancy is particularly large, indicating an effective magnetic field at the nucleus of 12 MG, as compared to an effective field of 3.3 MG observed in Sm metal. Such a large discrepancy in the observed effective field at the nucleus is difficult to understand even considering the large CEF effects evident in these materials. CEF effects are expected to have their major influence on the orbital angular momentum which is the principal source of the effective field at the nucleus in the rare-earth elements. In the case of $Ho_2Fe_3Si_5$, CEF effects may well result in a reduced effective magnetic field at the nucleus as indicated by the reduced nuclear Schottky anomaly in this compound.

No evidence can be found for superconductivity in the heat capacity of any of the antiferromagnetically ordered $M_2Fe_3Si_5$ compounds. In particular, superconductivity in $Tm_2Fe_3Si_5$ as has been reported based on inductance and resistivity measurements[9] is not supported by the heat-capacity results presented here. Based on previous heat-capacity measurements in $Lu_2Fe_3Si_5$, $Sc_2Fe_3Si_5$, and $Y_2Fe_3Si_5$, the jump in the heat capacity at the reported superconducting transition[9] of 1.7 K for $Tm_2Fe_3Si_5$ is expected to be less than 3% of the observed total heat capacity of $Tm_2Fe_3Si_5$ at 1.7 K and may therefore be unobservable in these data. Therefore, while the heat capacity of $Tm_2Fe_3Si_5$ in no way indicates superconductivity, the pos-

sibility of superconductivity in $Tm_2Fe_3Si_5$ cannot be entirely ruled out.

VI. SUMMARY

The low-temperature heat capacities of $M_2Fe_3Si_5$ compounds reveal a number of important features of the magnetic order in these compounds. In agreement with previous work,[5–8] no evidence for a magnetic moment on the Fe is found. The systematics of the ordering temperatures as determined calorimetrically (Fig. 9) indicate the principal mechanism by which the rare-earth atoms interact is the usual RKKY indirect exchange interaction. Several of these compounds exhibit multiple magnetic phase transitions, presumably due to the anisotropy and/or next-nearest-neighbor interactions. The conduction-electron–M interaction strength is on the order of 0.03 eV which, while much smaller than typical interaction energies in the rare-earth metals and binary intermetallic compounds, is larger than that observed in the ternary rhodium borides and the Chevrel-phase compounds which exhibit superconductivity in the presence of magnetic rare-earth atoms. No evidence for superconductivity can be found in the heat capacity of any of the $M_2Fe_3Si_5$ compounds involving rare-earth atoms with an incomplete $4f$ shell. This is attributed to the strength of the magnetic interactions.

The anomalous critical behavior observed in these materials is quite unusual. A first-order magnetic phase transition is indicated in $Er_2Fe_3Si_5$, and several other compounds exhibit critical behavior similar to that expected in mean-field theory. A linear term in the heat capacity of $Gd_2Fe_3Si_5$ below the antiferromagnetic transition temperature suggests the possibility of an unusual spin-wave dispersion relation in this material.

ACKNOWLEDGMENTS

The authors wish to thank A. R. Moodenbaugh for providing unpublished neutron-diffraction results on $Er_2Fe_3Si_5$ and H. F. Braun for useful correspondence. Ames Laboratory is operated for the U.S. Department of Energy by Iowa State University under Contract No. W-7405-Eng-82. This research was supported by the Director for Energy Research, Office of Basic Sciences.

[1]See, for example, *Superconductivity in Ternary Compounds,* edited by Ø. Fischer and M. B. Maple (Springer, Berlin, 1982), Vols. 1 and 2.

[2]H. B. MacKay, L. D. Woolf, M. B. Maple, and D. C. Johnston, J. Low Temp. Phys. 41, 639 (1980).

[3]H. R. Ott, L. D. Woolf, M. B. Maple, and D. C. Johnston, J. Low. Temp. Phys 39, 383 (1980).

[4]H. F. Braun, Phys. Lett. 75A, 386 (1980).

[5]J. D. Cashion, G. K. Shenoy, D. Niarchos, P. J. Viccaro, and C. M. Falco, Phys. Lett. 79A, 454 (1980).

[6]J. D. Cashion, G. K. Shenoy, D. Niarchos, P. J. Viccaro, A. T. Aldred, and C. M. Falco, J. Appl. Phys. 52, 2180 (1981).

[7]H. F. Braun, C. U. Segre, F. Acker, M. Rosenberg, S. Dey, and P. Deppe, J. Magn. Magn. Mater. 25, 117 (1981).

[8]A. R. Moodenbaugh, D. E. Cox, and H. F. Braun, Phys. Rev. B 25, 4702 (1981).

[9]C. U. Segre and H. F. Braun, Phys. Lett. 85A, 372 (1981).

[10]C. B. Vining, R. N. Shelton, H. F. Braun, and M. Pelizzone, Phys. Rev. B 27, 2800 (1983).

[11]L. J. Sundstrom, *Handbook on the Physics and Chemistry of Rare Earths,* edited by K. A. Gschneidner, Jr. and L. Eyring (North-Holland, Amsterdam, 1978), Vol. 1, p. 379.

[12]C. Domb, *Magnetism,* edited by G. K. Rado and H. Suhl (Academic, New York, 1965), Vol. IIA, p. 1.

[13]C. U. Segre, Ph. D. thesis, University of California at San Diego, La Jolla, 1981 (unpublished).

[14]A. R. Moodenbaugh, D. E. Cox, C. B. Vining, and C. U. Segre (unpublished).